Towards H$_2$-rich gas production from unmixed steam reforming of methane: Thermodynamic modeling

Aline Lima da Silva*, Iduvirges Lourdes Müller

Program of Postgraduate Studies in Mining, Metals and Materials Engineering (PPGEM), Federal University of Rio Grande do Sul – UFRGS, Campus do Vale, Setor 4, Prédio 75, Sala 226, Av. Bento Gonçalves 9500, CEP 91501-970, Porto Alegre, RS, Brazil

ARTICLE INFO

ABSTRACT

In this work, the Gibbs energy minimization method is applied to investigate the unmixed steam reforming (USR) of methane to generate hydrogen for fuel cell application. The USR process is an advanced reforming technology that relies on the use of separate air and fuel/steam feeds to create a cyclic process. Under air flow (first half of the cycle), a bed of Ni-based material is oxidized, providing the heat necessary for the steam reforming that occurs subsequently during fuel/steam feed stage (second half of the cycle). In the presence of CaO sorbent, high purity hydrogen can be produced in a single reactor. In the first part of this work, it is demonstrated that thermodynamic predictions are consistent with experimental results from USR isothermal tests under fuel/steam feed. From this, it is also verified that the reacted NiO to CH$_4$ (NiO$_{reacted}$/CH$_4$) molar ratio is a very important parameter that affects the product gas composition and decreases with time. At the end of fuel/steam flow, the reforming reaction is the most important chemical mechanism, with H$_2$ production reaching ~75 mol%. On the other hand, at the beginning of fuel/steam feed stage, NiO reduction reactions dominate the equilibrium system, resulting in high CO$_2$ selectivity, negative steam conversion and low concentrations of H$_2$. In the second part of this paper, the effect of NiO$_{reacted}$/CH$_4$ molar ratio on the product gas composition and enthalpy change during fuel flow is investigated at different temperatures for inlet H$_2$O/CH$_4$ molar ratios in the range of 1.2–4, considering the USR process operated with and without CaO sorbent. During fuel/steam feed stage, the energy demand increases as time passes, because endothermic reforming reaction becomes increasingly important as this stage nears its end. Thus, the duration of the second half of the cycle is limited by the conditions under which auto-thermal operation can be achieved. In absence of CaO, H$_2$ at concentrations of approximately 73 mol% can be produced under thermo-neutral conditions (H$_2$O/CH$_4$ molar ratio of 4, with NiO$_{reacted}$/CH$_4$ molar ratio at the end of fuel flow of ~0.8, in temperature range of 873–1073 K). In the presence of CaO sorbent, using an inlet H$_2$O/CH$_4$ molar ratio of 4 at 873 K, H$_2$ at concentrations over 98 mol% can be obtained all through fuel/steam feed stage. At 873 K, carbonation reaction provides all the heat necessary for H$_2$ production when NiO$_{reacted}$/CH$_4$ molar ratio reached at the end of fuel/steam feed is greater or equal to1. In this way, the heat released during air flow due to Ni oxidation can be entirely used to decompose CaCO$_3$ into CaO. In this case, a calcite-to-nickel molar ratio of 1.4 (maximum possible value) can be used during air flow. For longer durations of fuel/steam feed, corresponding to lower NiO$_{reacted}$/CH$_4$ molar ratios, some heat is necessary for steam reforming, and a calcite-to-nickel molar ratio of about 0.7 is more suitable. With the USR technology, CaO can be regenerated under air feeds, and an economically feasible process can be achieved.

1. Introduction

Hydrogen is considered to be an ideal clean energy carrier for the future because it is generally consumed as the fuel in low-temperature fuel cells, namely, proton exchange membrane fuel cells (PEMFCs). Over the years, much progress in PEMFCs has been implemented and this makes hydrogen production from the fuel processing of some feedstocks, such as fossil fuels and biomass, become increasingly important. Nowadays, 95% of the hydrogen production comes from steam reforming of natural gas, whose main component is methane. In addition to steam reforming, other thermo-chemical techniques including auto-thermal reforming (ATR) and (catalytic) partial oxidation (CPO or POX) have been regarded as efficient processes to hydrogen production [1–3]. In this context, unmixed steam reforming (USR) can be considered as an alternative process of catalytic steam reforming that relies

* Corresponding author. Tel.: +55 51 3308 9404.
E-mail address: adasilva26@gmail.com (A. Lima da Silva).

Nomenclature

G	total Gibbs energy of the system
G_i^0	Gibbs energy of species i at its standard state
n_i	number of moles of species i
y_i	mole fraction of species i
R	gas constant
T	temperature of the system
P	total pressure of the system
M, N	total number of components and species, respectively
α_{ik}	number of atoms of kth component present in each molecule of species i
b_k	total number of atomic masses of kth component in the system
ΔH	enthalpy change during fuel flow
in.	inlet
out.	outlet
Sel.	selectivity
Conv.	conversion
TN	thermo-neutral

on the use of separate air and fuel/steam feeds to create a cyclic process. Thus, the air and fuel/steam feeds do not mix, contrary to conventional ATR that uses pure oxygen for partial oxidation of the fuel to provide heat for the endothermic steam reforming reaction. Instead, USR makes use of an oxygen transfer material (OTM), which in its reduced form behaves as a steam reforming catalyst. In this study, Ni was chosen to be the OTM, since it is the most common catalyst for the steam reforming reactions and can be readily oxidized and reduced [4–11]. During USR, an air feed (first half of the cycle, in which Ni is converted into NiO) is followed by a fuel/steam feed (second half of the cycle, in which NiO regenerates to metallic Ni, and reforming reactions occur). Oxidation of the reduced catalyst under air flow is highly exothermic, thus generating the heat required by the endothermic steam reforming reactions that take place during the subsequent fuel/steam feed, and allowing the separation of inert N_2 from the reformate. Therefore, the USR process can run auto-thermally. Besides, the USR technology can be improved by introducing a CO_2-sorbent such as CaO into the reactor. In fact, calcite ($CaCO_3$) can be introduced along with Ni in the reactor. Under air flow, some heat released during Ni oxidation is utilized to thermally decompose calcite into CaO (calcination). In this way, the steam reforming reactions occur alongside CO_2 capture from the gas phase during the second half of the cycle. CaO reacts with CO_2 forming calcite again (carbonation). Consequently, water–gas shift (WGS) reaction is enhanced due to CO_2 adsorp-

tion, resulting in a decrease of the CO production, accompanied by an increase in H_2 concentration. The potential advantages of using CaO as a CO_2 acceptor have been previously demonstrated [12,13]. However, in order to obtain an economically feasible process, CaO has to be regenerated once it is fully converted to $CaCO_3$, and regeneration requires a certain amount of energy. Thus, the USR process offers a potential solution to this problem. While Ni oxidizes under the following air flow, some heat liberated is then utilized to decompose calcite to calcium oxide, regenerating the sorbent for the next cycle. In this way, under air flow, the reactor effluent is an oxygen-depleted and CO_2-rich air stream, whereas under fuel/steam feed, the gaseous species CO, CO_2 and H_2 evolve from the reactor. Based on the chemical reactions indicated in previous works [4,7,8], the main reactions involved in the unmixed steam reforming of methane can be summarized as depicted in Table 1. Under air feed, Ni on the catalyst support consumes oxygen via Ni oxidation to NiO generating heat (R-1) and the carbon deposits (formed in a previous fuel/steam feed) are burnt via complete (R-3) or partial oxidation (R-4). In the presence of calcite, some heat liberated in (R-1) allows the CaO sorbent to regenerate through calcination (R-2). Under fuel/steam feed, (R-6) is the global reaction that illustrates the OTM reduction with methane. While NiO is converted into Ni, significant carbon deposition may occur from fuel thermal decomposition (R-5). Once Ni is sufficiently reduced, methane steam reforming (R-9) occurs on the Ni catalyst, and water–gas shift reaction (R-10) takes place. In the presence of CaO sorbent, the reactions (R-6), (R-9) and (R-10) are followed by the carbonation reaction (R-11). Thus, the carbonation of the CaO sorbent allows not only the elimination of CO_2 from reformate, but also the shift of (R-6) and (R-10) to the right, enhancing the H_2 production. The USR process with CaO, as described in Fig. 1, was proposed in Ref. [7,14]. As can be seen, as nickel is cycled between NiO and catalytically active Ni, calcium is cycled between CaO and $CaCO_3$. The white regions are hotter from exothermic reactions (air flow) or heat storage (fuel/steam feed). USR first appeared in scientific literature through the publications of Kumar et al. [14] and Lyon and Cole [6]. More recently, Dupont et al. have experimentally investigated the production of hydrogen by USR of a variety of fuels, including methane [7,8], sunflower oil [8] and waste cooking oil [10,11]. The experimental results reported in these previous works indicate that USR is a promising fuel flexible technology able to produce fuel cell grade H_2 in a single reactor. Other advantages are claimed for the USR process, such as [6,7,14]: (i) economical at small scale, unlike the conventional process, which makes thus USR interesting for the use in distributed power generation; (ii) insensitivity to coking and sulfur (both could undergo oxidation under the air feed rather than irreversibly poisoning the reforming catalyst); (iii) potential for auto-thermal operation without the need for pure O_2 that would require a costly air separator; (iv) low cost reac-

Table 1
Summary of the main reactions of unmixed steam reforming process.

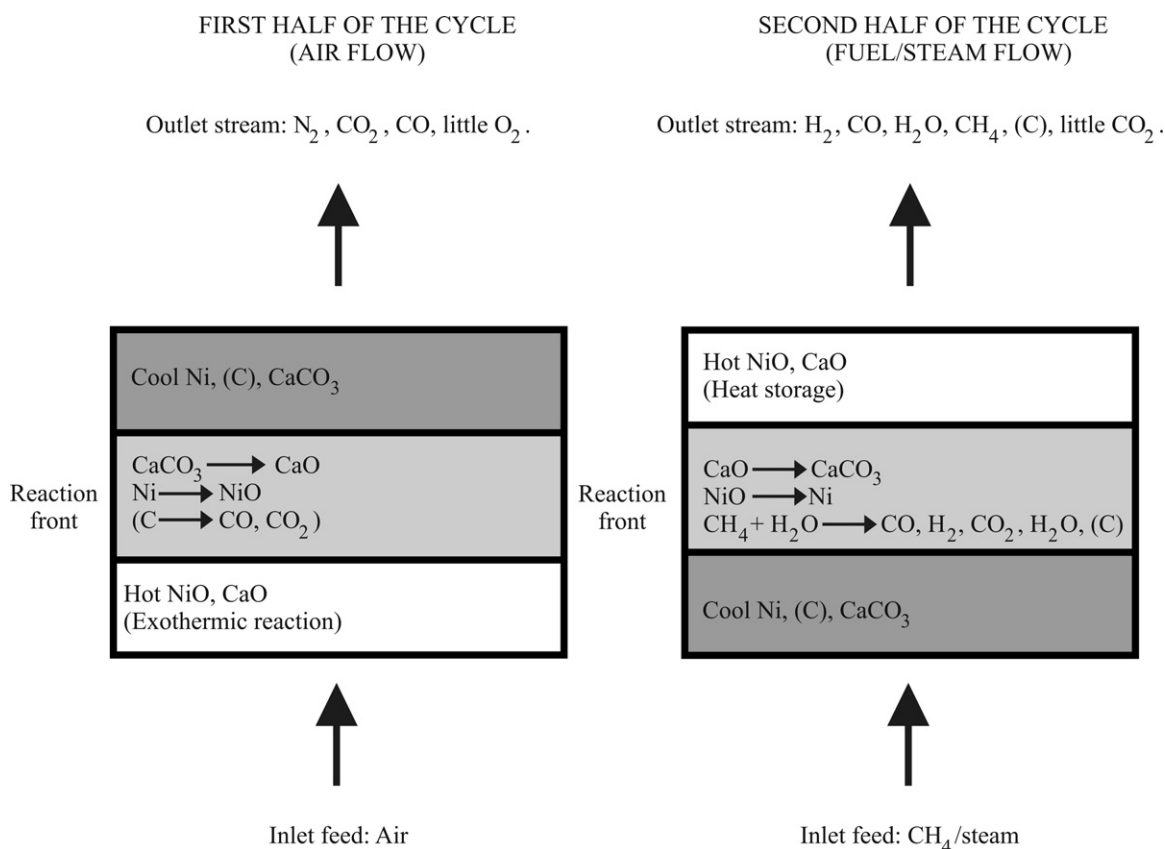| Half of the cycle	Reaction	Reaction type	ΔH_{298K}^0 ($\times 10^5$ J mol^{-1})
First: air feed (oxidizing mode)	$Ni + 0.5O_2 + 1.881N_2 \rightarrow NiO + 1.881N_2$ (R-1)	Oxidation of OTM and separation of N_2 from air	−2.39
	$CaCO_3 \rightarrow CaO + CO_2$ (R-2)	Thermal decomposition of calcite/regeneration of CaO sorbent	+1.79
	$C + O_2 \rightarrow CO_2$ (R-3)	Carbon complete oxidation	−3.93
	$C + 0.5O_2 \rightarrow CO$ (R-4)	Carbon partial oxidation	−1.10
Second: fuel/steam feed (reducing mode)	$CH_4 \rightarrow C + 2H_2$ (R-5)	Thermal decomposition of methane	+0.75
	$CH_4 + 4NiO \rightarrow CO_2 + 2H_2O + 4Ni$ (R-6)	Unmixed combustion of methane	+1.56
	$H_2 + NiO \rightarrow Ni + H_2O$ (R-7)	OTM reduction with H_2	−0.02
	$CO + NiO \rightarrow Ni + CO_2$ (R-8)	OTM reduction with CO	−0.44
	$CH_4 + H_2O \rightarrow CO + 3H_2$ (R-9)	Methane steam reforming	+2.06
	$CO + H_2O \rightarrow CO_2 + H_2$ (R-10)	Water–gas shift	−0.41
	$CaO + CO_2 \rightarrow CaCO_3$ (R-11)	Carbonation of CO_2 sorbent	−1.79
	$CH_4 + CaO + 2H_2O \rightarrow CaCO_3 + 4H_2$ (R-12)	Sorption enhanced reforming of methane	−0.14

FIRST HALF OF THE CYCLE
(AIR FLOW)

SECOND HALF OF THE CYCLE
(FUEL/STEAM FLOW)

Outlet stream: N_2, CO_2, CO, little O_2.

Outlet stream: H_2, CO, H_2O, CH_4, (C), little CO_2.

Cool Ni, (C), $CaCO_3$

$CaCO_3 \longrightarrow CaO$
Ni $\longrightarrow$ NiO
(C $\longrightarrow$ CO, CO_2)

Reaction
front

Hot NiO, CaO
(Exothermic reaction)

Inlet feed: Air

Hot NiO, CaO
(Heat storage)

CaO $\longrightarrow$ $CaCO_3$
NiO $\longrightarrow$ Ni
$CH_4 + H_2O \longrightarrow$ CO, H_2, CO_2, H_2O, (C)

Reaction
front

Cool Ni, (C), $CaCO_3$

Inlet feed: CH_4/steam

Fig. 1. Unmixed steam reforming process.

tor materials due to a hotter reactor center and colder walls, since USR allows the delivery of heat uniformly throughout a volume; (v) coupling of endothermic and exothermic reactions within a single reactor rather than relying on external heating, which ensures the compactness of the process. It is worth mentioning that the USR process offers similarities of chemical mechanism to chemical looping reforming (CLR). The term CLR, however, has been so far applied to interconnected fluidized beds through which the OTM circulates undergoing redox stages (see, for example, the references [4,5,9]). According to Dupont et al. [7], unmixed steam reforming is the term that could be used for the chemical looping reforming in a packed bed reactor.

Despite the relevance of such advanced reforming technology, there are only few papers dealing with the USR process. To the best of our knowledge, a comprehensive theoretical study dealing with the effect of the USR operating parameters on reformate composition has not yet been published. In this way, the present paper reports a detailed thermodynamic analysis of the methane unmixed steam reforming. Firstly, this work demonstrates that thermodynamic predictions are consistent with experimental results from USR isothermal tests under fuel/steam feed (CH_4/steam). The experimental data were compiled from Ref. [8]. Secondly, the effect of different parameters, like reactor temperature, inlet H_2O/CH_4, and $NiO_{reacted}/CH_4$ molar ratios, on the product gas composition and the conversions of CH_4 and H_2O is investigated for the USR process with/without calcium oxide. Additionally, an energy analysis is carried out, and the conditions for auto-thermal operation are identified. Finally, a summary of the optimized operating conditions under which H_2 production is maximized during auto-thermal USR is presented for both cases (with/without CO_2 acceptor). It is expected that the simulation results may provide an improved understanding of the chemical

mechanism involved in the USR process, specially of the effect that the $NiO_{reacted}/CH_4$ molar ratio has on the reformate composition and energy demand. Moreover, the results of the present study could aid in monitoring and designing new experiments.

2. Simulation methodology

For a system in which many simultaneous reactions take place, equilibrium calculations are performed through the Gibbs energy minimization method (non-stoichiometric approach). The total free energy of the system, composed of an ideal gas phase and pure condensed phases, may be expressed as

$$\frac{G}{RT} = \left(\sum_{i=1}^{N} n_i \left[\frac{G_i^0}{RT} + \ln(y_i P) \right] \right)_{gas} + \frac{1}{RT} \left(\sum_{i=1}^{N} n_i G_i^0 \right)_{condensed} \quad (1)$$

The problem consists in finding the different values of n_i which minimize the objective function given by Eq. (1), subject to the constraints of elemental mass balance

$$\sum_{i=1}^{N} n_i \alpha_{ik} = b_k, \quad k = 1, \ldots, M \quad (2)$$

In the non-stoichiometric approach, the species coexisting in the system at equilibrium must first be defined. For the USR of methane, under fuel/steam feed, the following species were considered: H_2, H_2O, CO, CO_2, CH_4 (ideal gas phase), C (graphite), Ni, and NiO (pure solid phases). In the presence of CO_2 sorbent, the following solid phases are also included in the compound basis set: CaO, Ca(OH)$_2$ and $CaCO_3$. The thermodynamic data necessary for describing the Gibbs energy of the species were obtained from Ref. [15].

The non-linear programming model comprising the objective function to be minimized and the constraints is solved by the Solver function contained in the Microsoft Excel spreadsheet package. In our previous works [12,16,17], the Solver function was shown to be a robust tool, able to solve convex non-linear optimization problems. A detailed explanation concerning the Generalized Reduced Gradient (GRG) algorithm and the use of the Solver function in equilibrium calculations can be seen in Ref. [16].

The present analysis was carried out over the following variable ranges: temperature of 873–1073 K, inlet H_2O/CH_4 molar ratio of 1.2–4 and $NiO_{reacted}/CH_4$ molar ratio of 0.12–3.12. In the presence of CaO sorbent, the inlet CaO/CH_4 molar ratio was of 1. For inlet H_2O/CH_4 molar ratios in the range of 1.2–4, it is found that graphite formation is suppressed. Thus, the simulations are performed in the carbon-free region. Even though carbon deposited during fuel flow can be burnt in the next air flow, and, thus, catalyst poisoning can be avoided, unlike conventional catalytic steam reforming, it remains desirable to prevent carbon deposition from the viewpoint of both optimizing heat transfer and achieving a maximum H_2 yield. Without carbon deposition, the heat transfer would be expected to move deeper in the reactor bed and allow better coupling of the exothermic and endothermic reactions [11].

Basic operating parameters for the USR process are the feed flow rate and the time duration of each feed stage [6]. The approach developed in the present work demonstrates that the time parameter monitored over fuel/steam feed stage (second half of the cycle) can be correlated to the $NiO_{reacted}/CH_4$ molar ratio to be used in the thermodynamic simulation. From the experimental values of CH_4 molar flow rate and the reduction molar rate of nickel oxide, it is possible to determine the $NiO_{reacted}/CH_4$ molar ratio to be considered as input parameter in the Gibbs energy minimization method. In this way, the experimental values recorded over the fuel/steam feed stage can be compared with the equilibrium data.

The steam conversion, given by

$$H_2O \ Conv. \ (\%) = 100 \times \frac{n_{H_2O,in} - n_{H_2O,out}}{n_{H_2O,in}}, \qquad (3)$$

and methane conversion efficiency, calculated by

$$CH_4 \ Conv. \ (\%) = 100 \times \frac{n_{CH_4,in} - n_{CH_4,out}}{n_{CH_4,in}}, \qquad (4)$$

are output parameters which, when maximized, could increase H_2 production, indicating a higher efficiency of the steam reforming reaction [8]. It is worth mentioning that, differently from the USR process, in the conventional steam reforming, steam conversion is not closely monitored and is rarely reported in the literature [7]. From Eq. (3), one can see that when steam conversion is negative, there is a net production of steam, when positive, there is a net consumption of steam.

Throughout this work, the selectivity of the carbon-containing products in the gas phase during fuel/steam feed stage was defined as:

$$Sel._{CH_4 \ or \ CO \ or \ CO_2}(\%) = 100 \times \frac{y_{CH_4 \ or \ CO \ or \ CO_2}}{y_{CH_4} + y_{CO} + y_{CO_2}} \qquad (5)$$

3. Results and discussion

3.1. Comparison with experimental values

In Fig. 2, it is possible to see the results obtained from two different experiments described in Ref. [8] along with thermodynamic equilibrium values computed in the present work. The experiments were performed at 1073 K, using an inlet H_2O/CH_4 molar ratio of 1.8 and different inlet molar flow rates of methane (1.13×10^{-4} and 3×10^{-4} mol s^{-1}). In all cases, the duration of fuel/steam feed

was 600 s. Fig. 2 shows H_2 concentration (a), CO and CO_2 selectivity (b), CH_4 and H_2O conversions (c), and experimental values of NiO reduction molar rate along with inlet methane molar flow rate (d). As can be seen, there is a time value (inferior axis) corresponding to each $NiO_{reacted}/CH_4$ molar ratio (superior axis). To obtain $NiO_{reacted}/CH_4$ molar ratio as a function of time, one should divide the experimental value of NiO reduction molar rate by the constant inlet molar flow rate of methane. From Fig. 2(d), one can easily see that NiO reduction molar rate sharply decreases with time in a packed bed reactor, indicating that the reduction reactions occur mainly at the beginning of fuel/steam feed. Since the reactor is fed by a constant molar flow rate of methane, $NiO_{reacted}/CH_4$ molar ratio also decreases with time. As can be seen in Fig. 2, thermodynamic results are in agreement with the experimental ones. At the beginning of fuel/steam feed ($NiO_{reacted}/CH_4$ molar ratio of 3), the reduction reactions (R-6)–(R-8) dominate the equilibrium system, resulting in high CO_2 selectivity, negative steam conversion and low concentrations of H_2 (40–50 mol%). However, as fuel/steam feed stage nears its end ($NiO_{reacted}/CH_4$ molar ratio of ~0.25), CO selectivity, steam conversion and H_2 concentration increase, whereas CO_2 selectivity decreases. This trend suggests that the reforming reaction (R-9) becomes much more important than the reduction reactions as time passes. At the end of fuel flow, CO selectivity is ~70%, steam conversion reaches a plateau of ~50%, and H_2 concentration is ~75 mol%. This behavior also indicates that H_2 production is limited by the equilibrium of reaction (R-10). Note that time axis starts in a value different from $t = 0$ s. In fact, there is an initial period, termed by Dupont et al. [8] as 'dead-time', under which thermal decomposition of methane plays an important role in the chemical mechanism, and hardly any output gases can be measured. In this initial period, H_2 concentration is close to zero, and significant carbon deposition occurs, resulting in disagreement with thermodynamic analysis, since at an inlet H_2O/CH_4 molar ratio of 1.8 at 1073 K graphite formation is thermodynamically inhibited. By the end of 'dead-time', carbon deposition is greatly reduced, as reported in Ref. [8]. In this way, the period corresponding to 'dead-time' is not shown in Fig. 2, because thermodynamic modeling does not apply to this early stage.

It is worth pointing out that, if the $NiO_{reacted}/CH_4$ molar ratio were neglected in the simulations, and only the inlet H_2O/CH_4 molar ratio and temperature were considered as input data in the Gibbs energy minimization method, discrepancies between thermodynamic predictions and experimental results could be seen. Fig. 3 shows the experimental data along with the results of the simulations carried out with/without $NiO_{reacted}/CH_4$ molar ratio as input parameter. As can be seen, when $NiO_{reacted}/CH_4$ molar ratio is not considered, H_2 concentration, CO selectivity and steam conversion are overestimated, whereas CO_2 selectivity is underestimated, mainly at the beginning of fuel/steam feed, because the effect of the reactions (R-6)–(R-8) is not taken into account. Therefore, it is evident that the reacted NiO to CH_4 molar ratio must be carefully determined from the operating parameters, such as inlet molar flow rate of methane, and experimental outputs, like NiO reduction molar rate, so that the thermodynamic equilibrium values can be satisfactorily compared with the experimental ones all through fuel/steam feed stage. de Diego et al. [4] carried out a thermodynamic analysis for the chemical looping reforming of methane in a circulating fluidized bed reactor. Taking into account the conversions reached by two different oxygen carriers (NiO18-αAl$_2$O$_3$ and NiO21-γAl$_2$O$_3$) and solid circulation flow rate, they estimated $NiO_{reacted}/CH_4$ molar ratios for these oxygen carriers. Thermodynamic calculations were also performed including $NiO_{reacted}/CH_4$ molar ratios. Interestingly, even working with different oxygen carriers which had different conversions during CLR, very similar gas composition at the outlet of the fuel reactor was obtained when $NiO_{reacted}/CH_4$ molar ratio was the same. Besides, the product
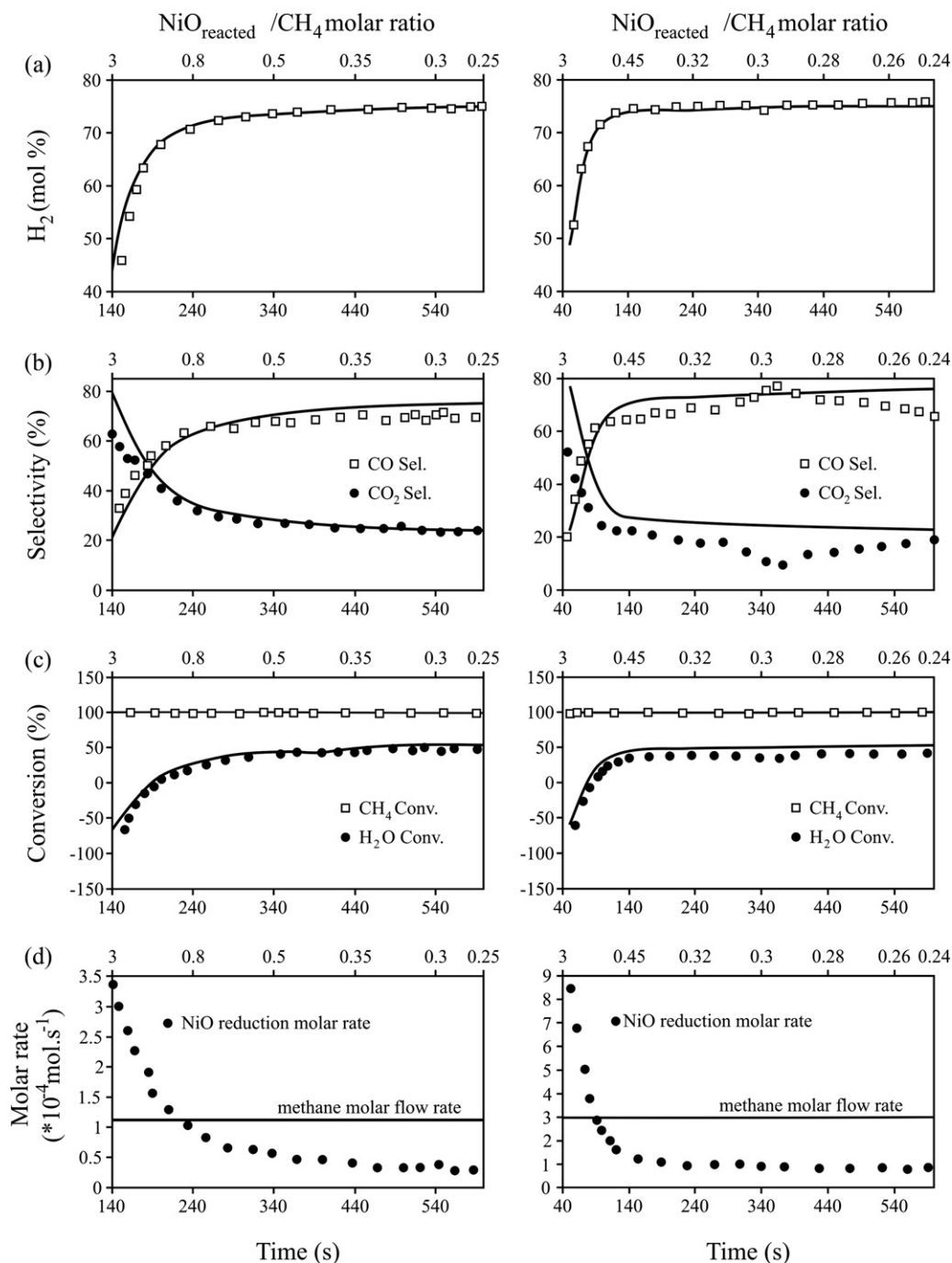
Fig. 2. (a) H_2 (mol%, dry basis), (b) CO and CO_2 selectivity, (c) CH_4 and H_2O conversion and (d) NiO reduction molar rate as a function of time. Markers: experimental data from [8]; solid lines: thermodynamic equilibrium data; methane molar flow rate used in the experiments: 1.13×10^{-4} (left plots) and 3×10^{-4} mol s^{-1} (right plots). Superior axis shows the NiO$_{reacted}$/CH_4 molar ratio corresponding to each time value.

gas compositions measured at the outlet of the fuel reactor were close to thermodynamic equilibrium. Thus, NiO$_{reacted}$/CH_4 molar ratio was found to be a suitable parameter to perform a thermodynamic analysis and compare results from different experiments with equilibrium values in a same diagram.

Obviously, for a given initial amount of NiO in a packed bed reactor and a fixed inlet flow rate of CH_4, thermodynamic analysis is not capable to predict NiO reduction molar rate as a function of time, because this depends on the kinetics of the gas-solid reaction. It is worth pointing out that, in Figs. 2 and 3, the product gas composition was presented as a function of time, because, at a given time t, NiO reduction molar rate is known from the experiments

of Ref. [8]. In this way, the NiO$_{reacted}$/CH_4 molar ratio corresponding to each time value can be easily estimated, and the equilibrium composition throughout the fuel/steam feed stage can be calculated. Thermodynamic calculations, besides of being a reliable tool to verify if the experimental values are consistent and plausible, are useful to evaluate how different parameters (temperature, inlet H_2O/CH_4 and NiO$_{reacted}$/CH_4 molar ratios) affect the production of H_2 and the energy demand of the USR process with and without CaO sorbent. Thus, the viability of producing high purity H_2 under auto-thermal operation with *in situ* sorbent regeneration is investigated by means of a thermodynamic study. The next sections are focused on the effect of these parameters on the product gas
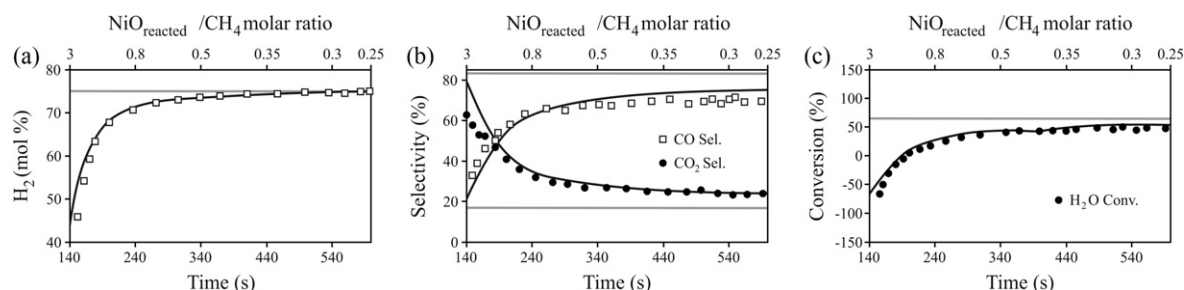
Fig. 3. (a) H_2 (mol%, dry basis), (b) CO and CO_2 selectivity, and (c) H_2O conversion as a function of time. Markers: experimental data from [8]; solid lines: results of the simulation with (black) and without (gray) $NiO_{reacted}/CH_4$ molar ratio as input parameter in the simulation. Experimental conditions from Ref. [8]: inlet $H_2O/CH_4 = 1.8$, $T = 1073$ K, methane molar flow rate (1.13×10^{-4} mol s^{-1}).

composition, CH_4 and H_2O conversions and enthalpy change during fuel/steam feed. The results are expressed in terms of a wide range of $NiO_{reacted}/CH_4$ molar ratios, because it is of interest to present generalized diagrams, which can be used as a benchmark to compare results from different experiments. Based on the results of Fig. 2, it was verified that $NiO_{reacted}/CH_4$ molar ratio decreases with time during fuel flow. In this way, the diagrams also indicate how product gas composition, H_2O and CH_4 conversions, and energy demand vary as time passes. Nevertheless, time values will depend on experimental conditions and kinetics. For example, in Fig. 2, for $NiO_{reacted}/CH_4$ molar ratio of ~3, thermodynamic and experimental results show that H_2 is obtained at a concentration of ~50 mol%. However, while this composition is reached at only 60 s in the case of the experiment performed with a methane inlet flow rate of 3×10^{-4} mol s^{-1}, for the experiment performed with a lower fuel flow rate (1.13×10^{-4} mol s^{-1}), this composition is achieved at ~160 s.

3.2. Effect of reactor temperature, inlet H_2O/CH_4 and $NiO_{reacted}/CH_4$ molar ratios in absence of CaO

Fig. 4 depicts the effect of $NiO_{reacted}/CH_4$ molar ratio on the concentrations (mol%, dry basis) of H_2 (a), CO (b), CO_2 (c) and the selectivity (%) of CO (d) and CO_2 (e), at 873, 973 and 1073 K for inlet H_2O/CH_4 molar ratios in the range of 1.2–4. At the beginning of fuel/steam feed stage ($NiO_{reacted}/CH_4$ molar ratio around 3), H_2 is found at low concentrations (35–45 mol%), with CO_2 being the major component of the gas phase (50–55 mol%), independently of inlet H_2O/CH_4 molar ratio and temperature. Note that, under these conditions, CO_2 selectivity is greater than 90% in all cases. This behavior suggests that, at the beginning of fuel flow, the OTM reduction reactions (R-6)–(R-8) are the main chemical mechanisms. However, as fuel/steam feed nears its end ($NiO_{reacted}/CH_4$ molar ratios ≤0.5), H_2 and CO concentration increase significantly. Thus, at the end of fuel flow, the endothermic reaction (R-9) is the main chemical mechanism. As can be seen, H_2 yield can be increased at the end of fuel/steam feed by using higher inlet H_2O/CH_4 molar ratios and more elevated temperatures, which is expected based on reaction (R-9). CO selectivity decreases with inlet H_2O/CH_4 molar ratio, whereas CO_2 selectivity increases, due to reaction (R-10). However, higher temperatures enhance CO production, because of the reverse water–gas shift reaction. The maximum H_2 content (~75%) is obtained at the inlet H_2O/CH_4 molar ratio equal to 4, with $NiO_{reacted}/CH_4$ molar ratio at the end of fuel/steam feed ≤0.5. Under these conditions, the main chemical mechanisms are the reactions (R-9) and (R-10), with minor effects of the reactions (R-6)–(R-8).

Fig. 5 shows the effect of $NiO_{reacted}/CH_4$ molar ratio on methane and steam conversions at 873 (a), 973(b) and 1073 K (c) for inlet H_2O/CH_4 molar ratios in the range of 1.2–4. As can be seen, at the beginning of fuel/steam feed, methane conversion is very high (>97%) and steam conversion is a negative value, independently of

temperature and inlet H_2O/CH_4 molar ratio. This can be attributed to reaction (R-6), which is a very important mechanism at the beginning of fuel flow. At 1073 K, methane conversion over 98% can be obtained all through fuel/steam feed, for inlet H_2O/CH_4 molar ratios in the range of 1.2–4. In this case, the endothermic reactions (R-6) and (R-9) are enhanced due to the elevated temperature. On the other hand, at 873 K, methane conversion decreases as time passes, mainly at low inlet H_2O/CH_4 molar ratios. This is due to the fact that steam reforming is not so favored at lower temperatures. At a given inlet H_2O/CH_4 molar ratio, steam conversion increases with operation time, because steam reforming becomes increasingly important as time passes. Besides, the highest steam conversions are achieved at higher temperatures, due to the endothermicity of the reforming reaction. Experimental results corroborate these findings. Dupont et al. [7] report that, at an inlet H_2O/CH_4 molar ratio of 1.8, CH_4 and H_2O conversions of 55 and 42%, respectively, are obtained at the end of fuel/steam feed at 873 K, whereas higher conversions of methane (99%) and steam (49%) are obtained at the end of fuel flow at 1073 K. In addition, it is worth pointing out that the highest steam conversions are reached with lower inlet H_2O/CH_4 molar ratios. Abundant water in the feed stream results in a great amount of non-reacted steam in the system.

3.3. Effect of reactor temperature, inlet H_2O/CH_4 and $NiO_{reacted}/CH_4$ molar ratios in the presence of CaO

The USR is meant to operate in the presence of a CO_2 sorbent [7]. Fig. 6 depicts the effect of $NiO_{reacted}/CH_4$ molar ratio on the concentrations (mol%, dry basis) of H_2 (a), CO (b), CO_2 (c) and CaO conversion (d) at 873 and 973 K, for inlet H_2O/CH_4 molar ratios in the range of 1.2–4. In all cases, a CaO/CH_4 molar ratio of 1 was used. At 873 K, with an inlet H_2O/CH_4 molar ratio of 4, H_2 can be produced at concentrations over 98 mol% all through fuel/steam feed. Accordingly, Fig. 6 (d) indicates that under these conditions CaO conversions reach values near 100%. On the other hand, with lower inlet H_2O/CH_4 molar ratios (e.g. 1.2), high purity H_2 is obtained during the initial stage of fuel flow, corresponding to higher $NiO_{reacted}/CH_4$ molar ratios. As time passes, and $NiO_{reacted}/CH_4$ molar ratio diminishes, H_2 concentration and CaO conversion decrease. At the end of fuel/steam feed, H_2 concentration is ~82 mol%, and CaO conversion is ~55%. At the beginning of fuel flow, complete CaO conversion and high purity H_2 are obtained at 873 K, independently of inlet H_2O/CH_4 molar ratio. From Fig. 4(e) at 873 K, it is observed that CO_2 selectivity is ~100% at the beginning of the process, due to reaction (R-6). Thus, very favorable conditions for the carbonation reaction (R-11) are achieved at the beginning of fuel flow. However, as fuel/steam feed approaches its end, CO_2 selectivity decreases. At the end of fuel flow, for an inlet H_2O/CH_4 molar ratio of 1.2, CO_2 selectivity is of only 10% at 873 K (see Fig. 4e). In this way, the results indicate that higher inlet H_2O/CH_4 molar
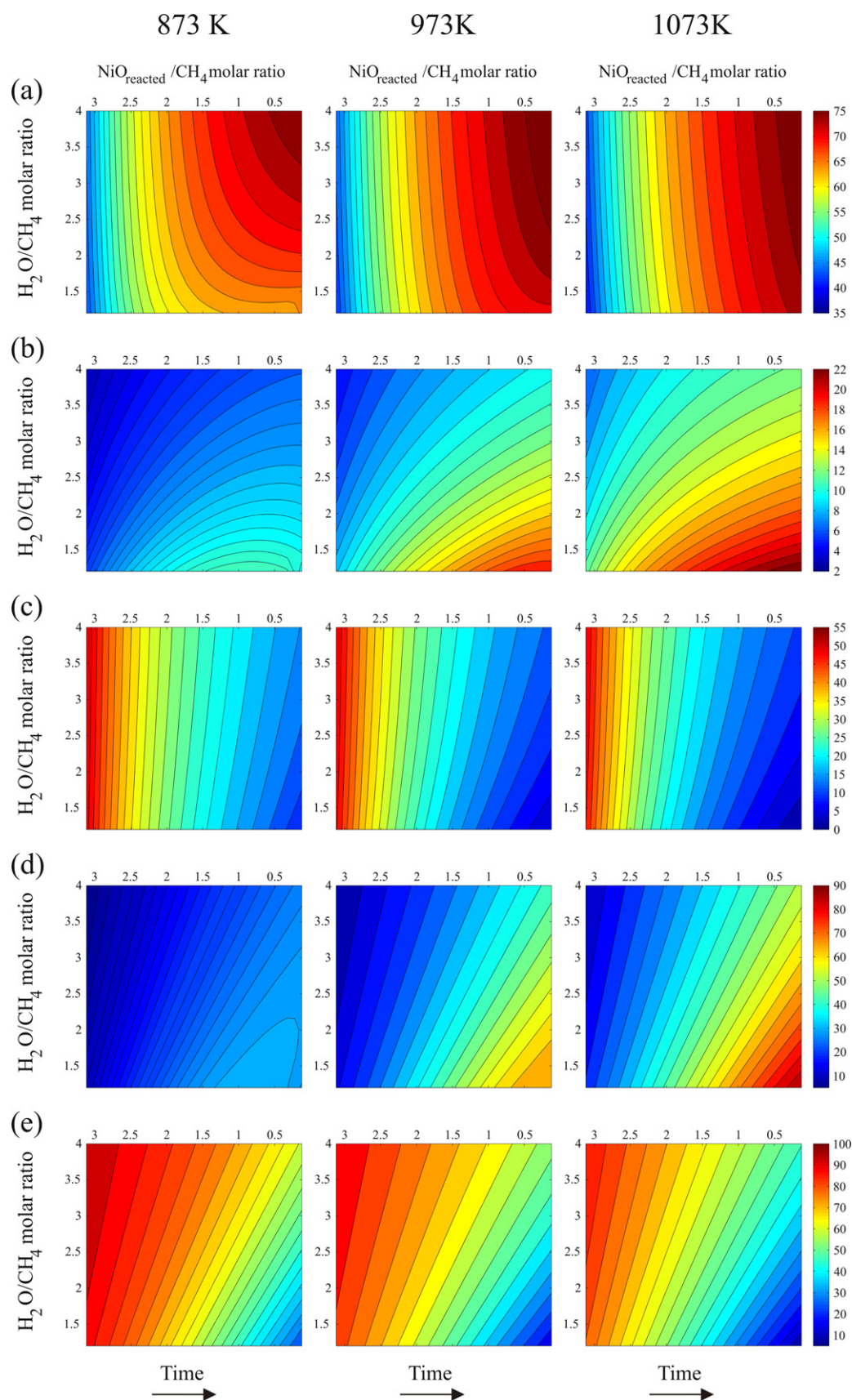
Fig. 4. H_2 (a), CO (b), CO_2 (c) concentration (mol%, dry basis) and CO (d), CO_2 (e) selectivity (%) as a function of inlet H_2O/CH_4 and $NiO_{reacted}/CH_4$ molar ratio at 873, 973 and 1073 K. Time duration of fuel/steam feed stage increases in the direction of the arrow.
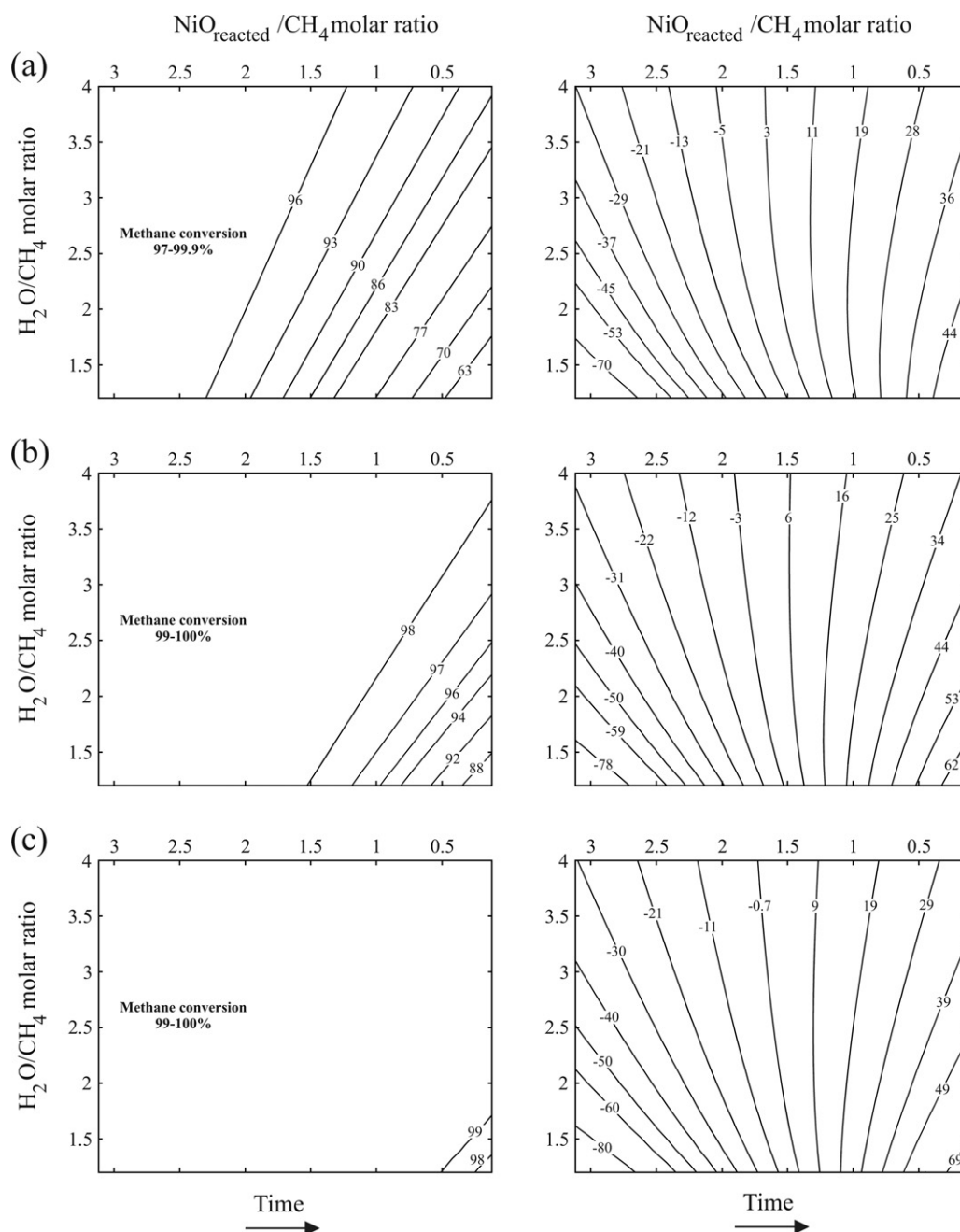
Fig. 5. Methane (left plots) and steam conversions (right plots), in %, as a function of inlet H_2O/CH_4 and $NiO_{reacted}/CH_4$ molar ratio at 873 (a), 973 (b) and 1073 K (c). Time duration of fuel/steam feed stage increases in the direction of the arrow.

ratios are suitable to produce H_2 during long periods at 873 K. In fact, reaction (R-12) shows that hydrogen production is enhanced with increasing steam in the feedstock. Nevertheless, in practice, the period of H_2-rich gas production depends on CO_2 breakthrough curve of the sorbent. Due to the fixed amount of sorbent in an experimental run, CO_2 concentration in the product gas raises rapidly once the sorbent reaches a certain capacity. This is termed CO_2 breakthrough [18]. During the pre-CO_2 breakthrough period, high purity H_2 is produced. By comparing Figs. 4(b) vs. 6(b) and Figs. 4(c) vs. 6(c), one can see that CO and CO_2 concentrations are enormously decreased in the presence of CaO sorbent. In absence of CaO, CO and CO_2 concentrations of ~12 and 55%, respectively, can be reached at 873 K, whereas in the presence of CO_2-acceptor, both CO and CO_2 concentrations are inferior to 1.6%. Unlike the process at 873 K, in which high purity H_2 is produced in a wide

range of inlet H_2O/CH_4 and $NiO_{reacted}/CH_4$ molar ratios, Fig. 6(a) shows that at 973 K the region of high concentrations of H_2 is much narrower. Thus, at 973 K, H_2-rich gas is produced during shorter periods than at 873 K. Besides, the maximum H_2 concentration achieved at 973 K is ~90 mol%. Indeed, the exothermic carbonation (R-11) is not favored with temperature and, as a consequence, CaO conversion diminishes (compare Fig. 6(d) – 873 K vs. 973 K). Moreover, at 973 K, CO and CO_2 can be found at concentrations of approximately 16 mol%.

Methane and steam conversions are higher in the presence than in absence of CaO sorbent. This effect is noteworthy at 873 K. By comparing Figs. 5(a) vs. 7(a), one can see that, in the presence of CaO, using an inlet H_2O/CH_4 molar ratio greater than 3.5, the region of maximum methane conversion (>97%) can be extended until the end of fuel/steam feed (lower $NiO_{reacted}/CH_4$ molar ratios), due to
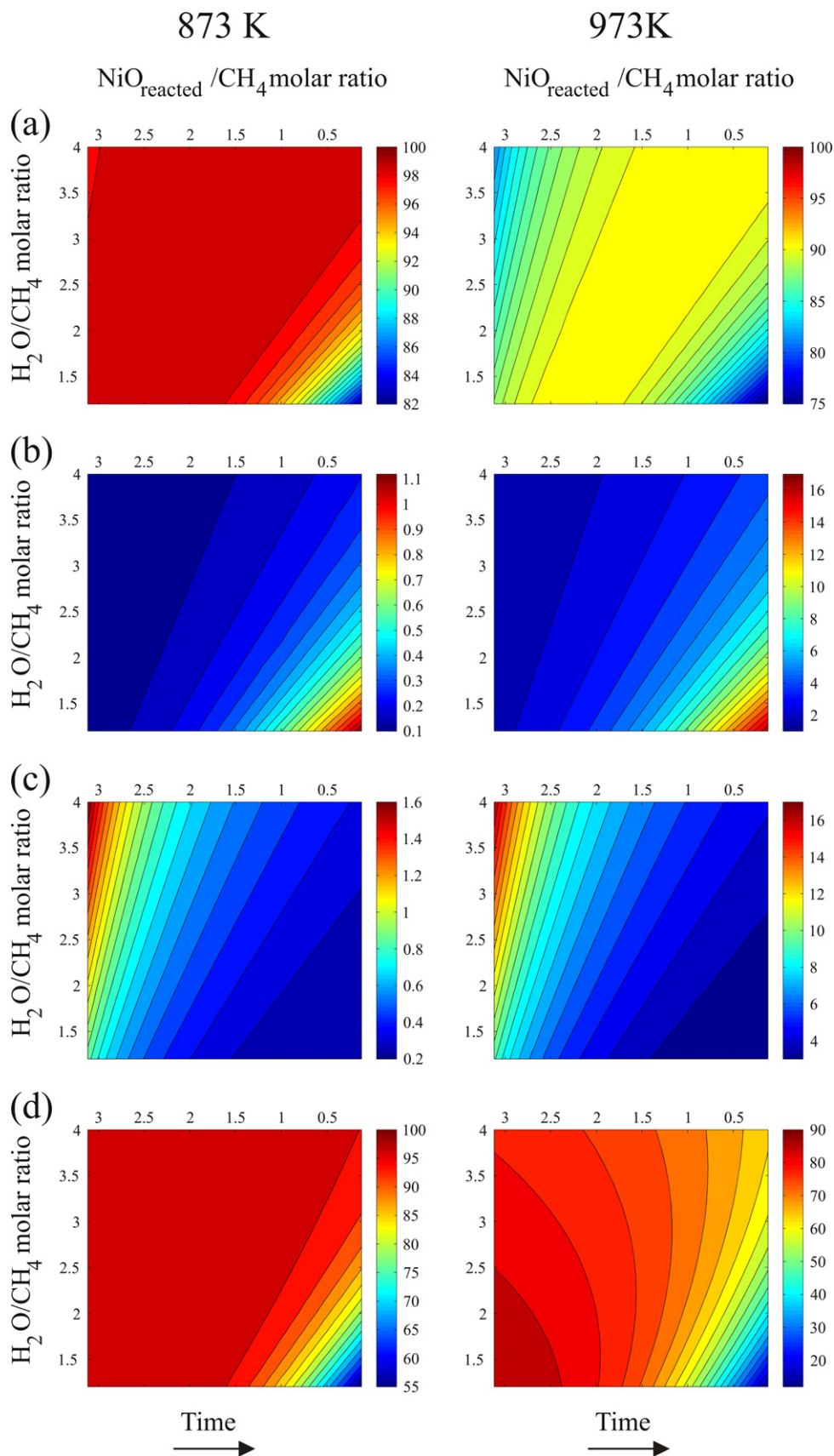
Fig. 6. H_2 (a), CO (b), CO_2 (c) concentration (mol%, dry basis) and CaO conversion (d) as a function of inlet H_2O/CH_4 and $NiO_{reacted}/CH_4$ molar ratio at 873 and 973 K. CaO/CH_4 molar ratio = 1. Time duration of fuel/steam feed stage increases in the direction of the arrow.
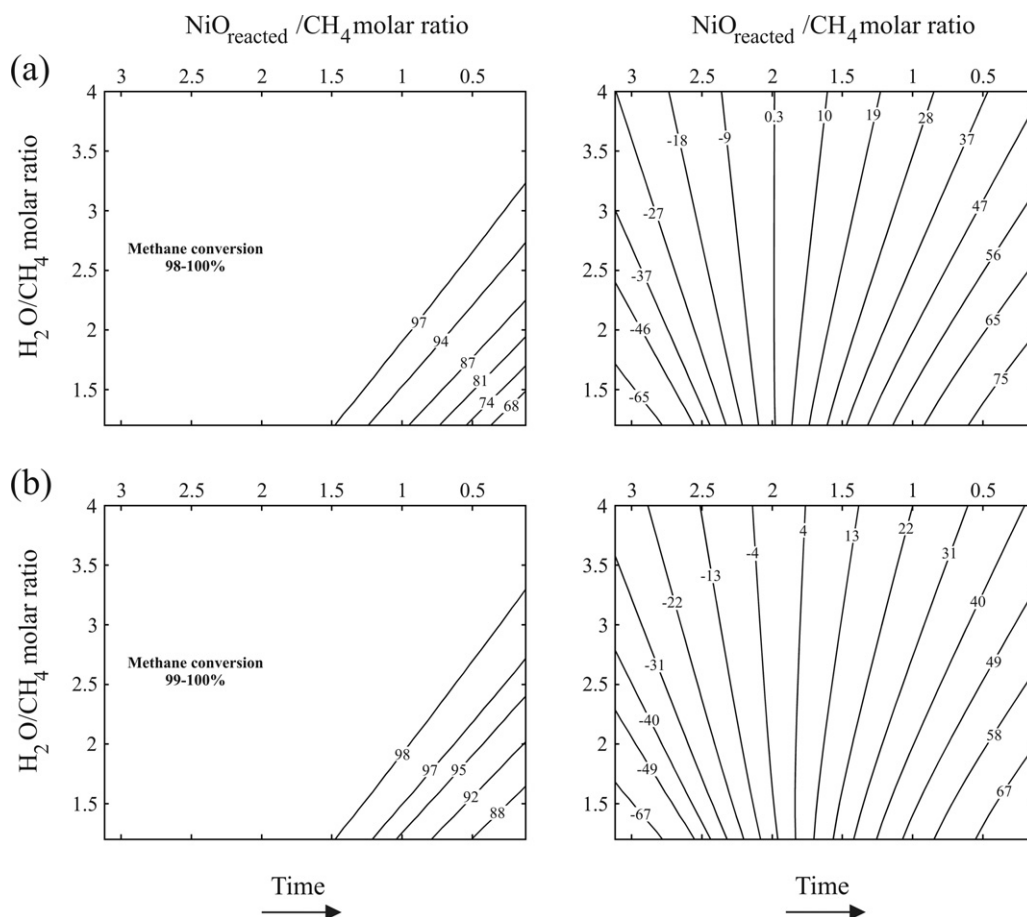
Fig. 7. Methane (left plots) and steam conversions (right plots), in %, as a function of inlet H_2O/CH_4 and $NiO_{reacted}/CH_4$ molar ratio at 873 (a) and 973 K (b). CaO/CH_4 molar ratio = 1. Time duration of fuel/steam feed stage increases in the direction of the arrow.

the enhanced reforming process. Besides, the maximum steam conversion reached in a process with CO_2-acceptor is much greater than that without CaO sorbent, *i.e.* 75% instead of 44%.

3.4. Molar composition during fuel/steam stage

Fig. 8 depicts the effect of $NiO_{reacted}/CH_4$ molar ratio on the moles of H_2 (a), CO_2 (b), CO (c) and H_2O (d) at 873 K, for inlet H_2O/CH_4 molar ratios in the range of 1.2–4, in a process without (left graphs) and with (right graphs) CaO sorbent. As can be seen, the number of moles of H_2 increases as time passes, because steam reforming becomes increasingly important with decreasing $NiO_{reacted}/CH_4$ molar ratio. In the presence of CaO sorbent, for inlet H_2O/CH_4 molar ratios >3, the number of moles of H_2 approaches 4 (3.7 mol H_2 per mol of CH_4), which is in agreement with reaction (R-12). At the beginning of fuel/steam feed stage, the inlet H_2O/CH_4 molar ratio exerts almost no influence on the number of moles of H_2. Under these conditions, the number of moles of H_2 is very low, due to reaction (R-7), which is favored at high $NiO_{reacted}/CH_4$ molar ratios. In fact, as can be seen in Fig. 8(d), there is a great steam production due to OTM reduction at the beginning of fuel flow. In absence of CaO sorbent, the number of moles of CO_2 is approximately 1 at the beginning of fuel flow, indicating that unmixed combustion of methane (reaction (R-6)) is an important chemical mechanism in the initial stages. In the presence of CaO, the number of moles of CO_2 is close to zero, independently of $NiO_{reacted}/CH_4$ molar ratio, which means that CO_2 is removed from the gas phase by the reaction (R-11) all through fuel/steam feed. The number of moles of CO increases as fuel/steam stage nears its end, because

reaction (R-9) is the most important mechanism at the end of the fuel stage. Besides, CO is favored at lower inlet H_2O/CH_4 molar ratios, due to the reverse of water–gas shift reaction. The number of moles of CO in a process with CaO sorbent is much lower than that in a process without CaO, because of the enhanced water–gas shift reaction (R-10).

Fig. 9 depicts the effect of $NiO_{reacted}/CH_4$ molar ratio on the moles of H_2 (a), CO_2 (b) and CO (c) at 973 K, for inlet H_2O/CH_4 molar ratios in the range of 1.2–4, in a process without (left graphs) and with (right graphs) CaO sorbent. As can be observed, the trends of the number of moles of species with $NiO_{reacted}/CH_4$ molar ratio are the same as those shown in Fig. 8. In the presence of CaO, the number of moles of CO_2 and CO at 973 K is greater than at 873 K. This is due to the fact that the reaction (R-11) is exothermic and, thus, more favored at lower temperatures. Consequently, in a sorption enhanced reforming process, the number of moles of H_2 at 973 K is lower than at 873 K. In absence of CaO, by comparing Fig. 8 vs. Fig. 9, one can see that, at higher temperatures, the number of moles of H_2 and CO increase, due to endothermicity of reaction (R-9), whereas the number of moles of CO_2 decreases, because of the reverse of reaction (R-10).

3.5. Energy analysis

The USR process should be carried out as close to auto-thermal as possible, that is, with little or any heat being supplied to the reactor [11]. Table 2 depicts the input conditions and outputs for the auto-thermal operation of the methane USR. The amounts of reactants were calculated taking into account the thermo-neutral
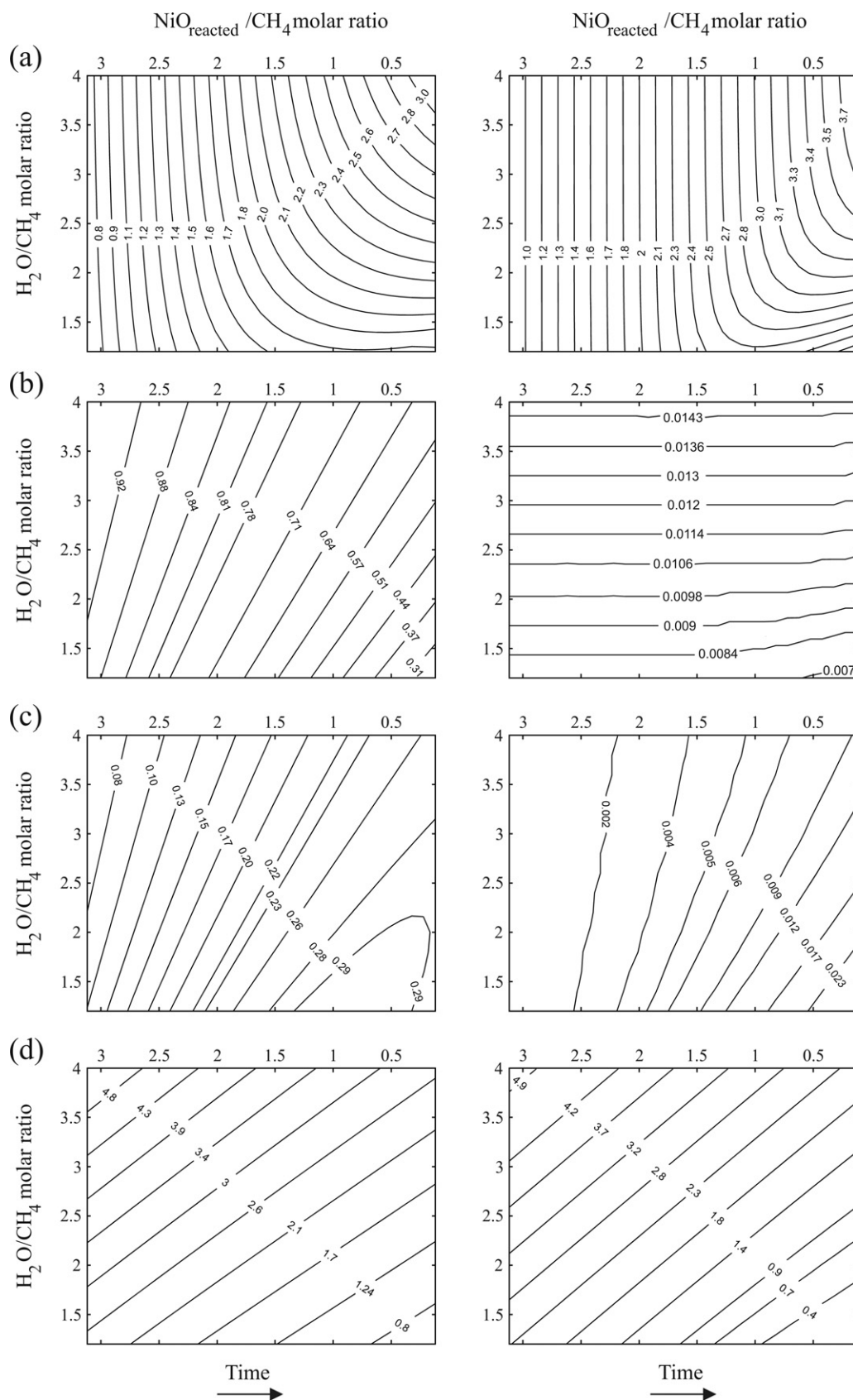
Fig. 8. Moles of species per mol of methane as a function of inlet H_2O/CH_4 and $NiO_{reacted}/CH_4$ molar ratio at 873 K. (a) H_2, (b) CO_2, (c) CO and (d) H_2O. Left contour plots: USR without CaO sorbent. Right contour plots: USR with CaO sorbent (CaO/CH_4 molar ratio = 1). Time duration of fuel/steam feed stage increases in the direction of the arrow.

Fig. 9. Moles of species per mol of methane as a function of inlet H_2O/CH_4 and $NiO_{reacted}/CH_4$ molar ratio at 973 K. (a) H_2, (b) CO_2, and (c) CO. Left contour plots: USR without CaO sorbent. Right contour plots: USR with CaO sorbent (CaO/CH_4 molar ratio = 1). Time duration of fuel/steam feed stage increases in the direction of the arrow.
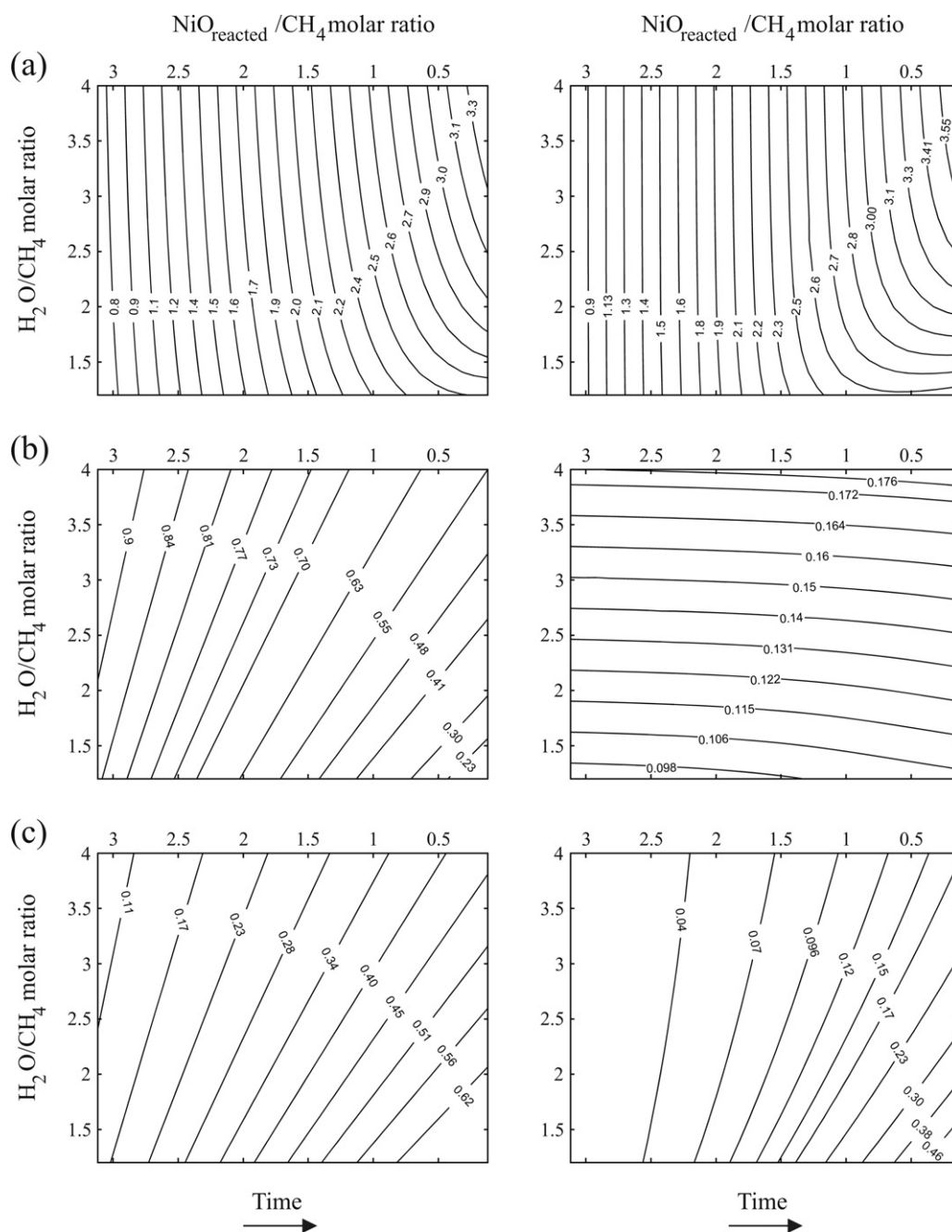
Table 2
Thermodynamic equilibrium results for USR process (with/without CaO sorbent) and comparison of USR (without sorbent) with ATR under thermo-neutral conditions.

Reforming technology	T (K)	Inlet molar ratio	Conversion (%)	H_2 (dry basis, %)	CO selectivity	CO_2 selectivity	ΔH (J mol^{-1}) (reactant)
(1) USR-fuel flow	1073	$NiO_{reacted}/CH_4 = 0.84$ $H_2O/CH_4 = 4$	H_2O: 18.33 CH_4: 99.97	73.21	42.59	57.37	2.334×10^5 (NiO)
(2) USR-air flow	1273	$O_2/Ni = 0.5$ $N_2/Ni = 1.881$	Ni: 100 O_2: 100	–	–	–	-2.336×10^5 (Ni)
(3) ATR thermo-neutral conditions	1073	$O_2/CH_4 = 0.42$ $H_2O/CH_4 = 4$	H_2O: 18.33 CH_4: 99.97	73.21	42.59	57.37	-0.01×10^5 (CH_4)
(1) USR-fuel flow with CaO sorbent	873	$NiO_{reacted}/CH_4 = 0.22$ $H_2O/CH_4 = 4$ $CaO/CH_4 = 1$	H_2O: 43.73 CH_4: 98.90 CaO: 96.54	99.08	25.54	42.38	0.737×10^5 (NiO)
(2) USR-air flow with $CaCO_3$	1273	$O_2/Ni = 0.5$ $N_2/Ni = 1.881$ $CaCO_3/Ni = 0.958$	Ni: 100 O_2: 100 $CaCO_3$: 100	–	–	–	-0.733×10^5 (Ni)
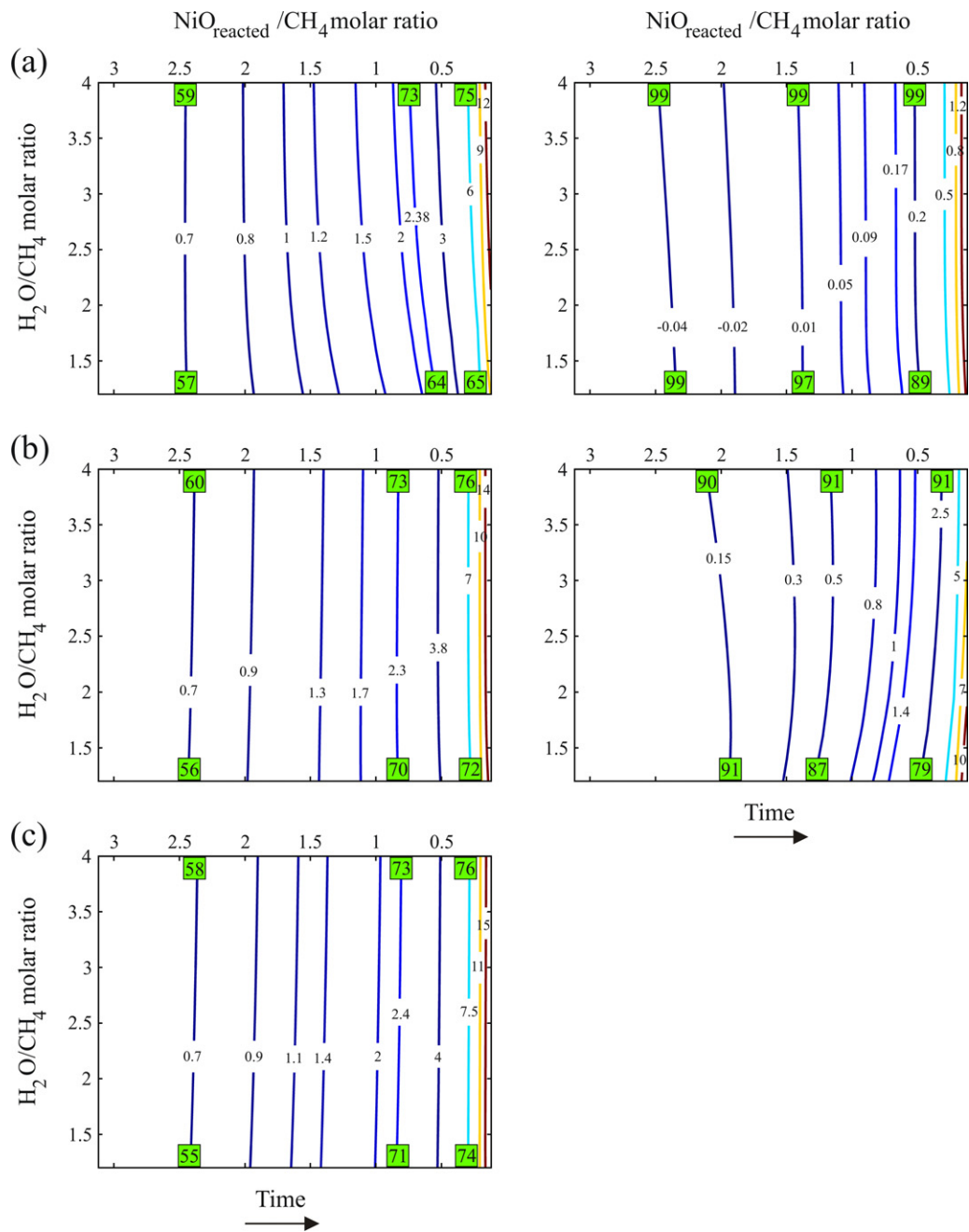
Fig. 10. Enthalpy change ($\times 10^5$ J mol^{-1} (NiO)) as a function of inlet H_2O/CH_4 and $NiO_{reacted}/CH_4$ molar ratio at 873 (a), 973 (b) and 1073 K (c). Left contour plots: USR without CaO sorbent. Right contour plots: USR with CaO sorbent (CaO/CH_4 molar ratio = 1). H_2 concentration (mol%, dry basis) is indicated at inlet H_2O/CH_4 molar ratios of 1.2 and 4. Time duration of fuel/steam feed stage increases in the direction of the arrow.

Table 3

Process outputs under optimized conditions; maximum H_2 concentration produced during auto-thermal methane USR with/without CaO.

T (K)	Without CaO			With CaO			
	873	973	1073	873		973	
Inlet H_2O/CH_4 molar ratio		4				4	
$NiO_{reacted}/CH_4$ molar ratio at the end of fuel/steam feed	0.76	0.82	0.84	1.22	0.12	1.82	1.02
H_2 (mol%, dry basis)	73.4	73.8	73.2	99	99	90	91
CO (mol%, dry basis)	6.1	9.1	11.4	0.16	0.25	2.5	3.1
CO_2 (mol%, dry basis)	18.9	17	15.4	0.5	0.4	5.6	7.5
CH_4 conversion (%)	93.6	99.6	99.9	99	99	99	99
H_2O conversion (%)	22.1	20.7	18.3	19	46	3	22
ΔH ($\times 10^5$ J mol^{-1} (NiO))	2.32	2.34	2.34	0.03	1.2	0.21	0.56
Inlet $CaCO_3$/Ni under air flow	–	–	–	1.4	0.7	1.3	1.1
Moles of graphite	–	–	–	–	–	–	–

conditions, that is, conditions under which the enthalpy change during fuel flow (ΔH), generally endothermic, is of the same magnitude of the heat released during air flow. Note that an adiabatic process is assumed. Additionally, a comparison of the USR (without sorbent) with the conventional ATR process under thermo-neutral conditions is shown. As can be seen, USR and ATR produce the same output (gas composition and conversions) on a same inlet H_2O/CH_4 molar ratio. The oxidation of the nickel catalyst is exothermic (-2.34×10^5 J mol^{-1}), and the heat necessary to decompose calcite through (R-2) is endothermic (+1.673 $\times 10^5$ J mol^{-1} at 1273 K). Therefore, for a $CaCO_3$/Ni molar ratio of 1.4, the oxidation of Ni provides the total amount of heat required to decompose $CaCO_3$ into CaO. In the specific case illustrated in Table 2 for the USR process with CaO sorbent, one can see that, during fuel flow, a heat input of +0.737 $\times 10^5$ J mol^{-1} is necessary. As some heat is needed for the reforming process, the $CaCO_3$/Ni molar ratio should be lower, *i.e.* of 0.958 instead of 1.4. It is worth mentioning that, by adding the CaO sorbent, it is possible to change the steam reforming reaction from an equilibrium that is strongly endothermic to one that is weakly exothermic [6], because of the exothermicity of carbonation reaction (R-11). When the heat for the steam reforming process is completely provided by the carbonation reaction ($\Delta H \sim 0$), the heat released during air flow can be entirely used to decompose the $CaCO_3$ into CaO. Consequently, the $CaCO_3$/Ni molar ratio of 1.4 can be used. It is worth pointing out that, when in auto-thermal operation, the reactor temperature oscillates during each cycle, with the lowest temperatures during the fuel feed and the highest at air flow [7]. In this work, the temperature at air flow is assumed to be 1273 K. Thus, the heat released during Ni oxidation is 2.34 $\times 10^5$ J mol^{-1}.

Fig. 10 shows the enthalpy change during fuel flow as a function of the inlet H_2O/CH_4 and $NiO_{reacted}/CH_4$ molar ratio, without (left graphs) and with (right graphs) CaO sorbent, at 873 (a), 973(b) and 1073 K (c). At 1073 K, carbonation reaction is not favored. As a general trend, the energy demand is lower at the beginning of fuel/steam feed and increases continuously as time passes. At the beginning of fuel flow ($NiO_{reacted}/CH_4$ molar ratios >2.5), the exothermic reduction reactions (R-7) and (R-8) are favored. On the other hand, as fuel flow nears its end ($NiO_{reacted}/CH_4$ molar ratios <0.5), the endothermic steam reforming reaction (R-9) becomes the main chemical mechanism. In absence of CaO sorbent, energy demand at the end of fuel flow is high and increases with temperature due to the endothermicity of steam reforming (12, 14 and 15 $\times 10^5$ J mol^{-1}, at 873, 973 and 1073 K, respectively). Note that hydrogen concentration also increases with time. However, the USR process should be carried out as close to auto-thermal as possible. In this way, the maximum concentration of H_2 is limited by thermo-neutral conditions, *i.e.*, the enthalpy change during fuel flow should be around 2.34 $\times 10^5$ J mol^{-1}. As can be seen, with an inlet H_2O/CH_4 molar ratio of 4, H_2 at a concentration of 73 mol% can be obtained under these conditions. Therefore, longer operation times would result in high energy demand, with H_2 concentration being increased only slightly. In the presence of CaO sorbent, due to the exothermic carbonation reaction (R-11), the energy demand is much lower than that of the process without CaO. In fact, at 873 K, the energy demand is lower than 2.34 $\times 10^5$ J mol^{-1} (NiO) all through fuel/steam feed. Thus, some heat released during air flow can be used to decompose $CaCO_3$ into CaO. If $NiO_{reacted}/CH_4$ molar ratio reached at the end of fuel/steam feed is low (e.g. 0.12), the energy demand during fuel flow is ~1.2 $\times 10^5$ J mol^{-1} (NiO). Thus, a $CaCO_3$/Ni molar ratio of ~0.7 can be used during air feed, in order to achieve an overall auto-thermal operation. If the duration of fuel/steam feed is not so long, and $NiO_{reacted}/CH_4$ molar ratio reached at the end of fuel flow is greater (~1.22), the enthalpy change during fuel/steam feed is near zero (0.05 $\times 10^5$ J mol^{-1} (NiO)), which means that the heat required for

steam reforming is completely provided by the carbonation reaction. In this way, a $CaCO_3$/Ni molar ratio of 1.4 (maximum possible value) can be used during air flow. These results indicate that high purity H_2 can be produced in an auto-thermal process, in which the sorbent is regenerated under air feeds. Interestingly, for the USR process operated with CaO sorbent at 873 K, it is found that weakly exothermic conditions are achieved at the beginning of the flow. As stated in the section 3.2, CO_2 selectivity is initially very high, due to reaction (R-6). Under these conditions, the exothermic reaction (R-11) is greatly favored, resulting in an exothermic equilibrium. At 973 K, the carbonation reaction is less favored than at 873 K. In this way, the energy demand at 973 is greater than that at 873 K.

3.6. Summary of the best operational conditions for the USR of methane

Table 3 shows the optimal conditions for the methane USR process with and without CaO sorbent. As can be seen, high H_2 concentrations can be reached under thermo-neutral conditions, with no carbon deposition during fuel flow. In absence of CaO, the reformate composition is suitable to feed the anode of solid oxide fuel cells (SOFC) or molten carbonate fuel cells (MCFC), which are more tolerant to other syngas compounds, and H_2 purity may not be so critical. For PEMFCs application, whose anode must be fueled by a high purity hydrogen stream containing CO at concentrations lower than 20 ppm to avoid platinum catalyst poisoning, the USR process should be operated with CaO in order to produce a H_2-rich gas. Besides, an additional step, including a COPROX (preferential CO oxidation) reactor, is also needed.

As can be seen in Table 3, it is possible to obtain H_2 at concentrations of about 99% at 873 K, using an inlet H_2O/CH_4 molar ratio of 4. During isothermal tests in the presence of a CO_2-sorbent, it is reported that H_2 contents above 90% can be obtained, using the same amount of water in the feed stream at 873 K [8]. Auto-thermal operation should be experimentally investigated for the methane USR process. More recently, Dupont et al. [11] reported catalyst and CO_2-sorbent regeneration, along with long periods of auto-thermal operation, for the USR process with waste cooking oil as a fuel.

4. Conclusions

The Gibbs energy minimization method is applied to investigate the unmixed steam reforming (USR) of methane to generate hydrogen for fuel cell application. The following conclusions can be drawn from the results of the present study:

- The methodology works in the region after the 'dead time'. After the initial period known as 'dead time', under which thermal decomposition of methane plays an important role in the chemical mechanism, and hardly any output gases can be measured, the experimental values of H_2 concentration, CO and CO_2 selectivities, and CH_4 and H_2O conversions approach the thermodynamic predictions. The methodology developed in the present study allows that the time parameter monitored over fuel/steam feed stage can be correlated to the $NiO_{reacted}/CH_4$ molar ratio to be used as input data in thermodynamic simulations. For a constant inlet molar flow rate of methane in a packed bed reactor, NiO reduction molar rate decreases as time passes. In this way, $NiO_{reacted}/CH_4$ molar ratio also decreases with time. Thermodynamic shows that, with decreasing $NiO_{reacted}/CH_4$ molar ratio, H_2 concentration, CO selectivity and steam conversion gradually increase, whereas CO_2 selectivity decreases. This behavior indicates that, as fuel/steam feed nears its end, the reforming reaction becomes increasingly important, with H_2 production limited by

the water–gas shift reaction. On the other hand, at the beginning of fuel/steam feed stage, the effect of the reactions involving NiO reduction is greater, resulting in low production of H_2 and high concentrations of CO_2 and H_2O.

- Thermodynamic calculations showed to be a reliable tool to verify if the experimental values are consistent and plausible. Besides, the results of the present work contribute towards a better understanding of the behavior of the product gas composition and enthalpy change during fuel/steam stage. Nevertheless, further investigations, including kinetics and reactor modeling, are encouraged to provide an accurate estimative of NiO reduction molar rate and output gas composition as a function of time.

- In absence of CaO sorbent, H_2-rich gas without carbon deposition can be obtained at inlet H_2O/CH_4 molar ratios greater than 1.2, with $NiO_{reacted}/CH_4$ molar ratios ≤ 0.5. Under these conditions, steam reforming is the main chemical mechanism, and H_2 at concentrations of 74–75 mol% can be produced. However, as time passes during fuel/steam feed stage, $NiO_{reacted}/CH_4$ molar ratio decreases, and, consequently, the overall process becomes increasingly endothermic, since the reforming reaction becomes more important than exothermic reduction reactions. In this way, the heat released during air flow may not be sufficient to supply the energy demand needed to produce H_2 at the highest concentrations. The duration of fuel/steam feed is limited by the conditions under which auto-thermal operation can be achieved. Thus, the maximum H_2 concentration that can be reached under thermo-neutral conditions (H_2O/CH_4 molar ratio of 4 and $NiO_{reacted}/CH_4$ molar ratio at the end of fuel/steam feed of ~ 0.8) is approximately 73 mol%.

- Unlike the USR process operated without CaO sorbent, in which H_2 concentration gradually increases with time, thermodynamic results indicate that, in the presence of CaO, using an inlet H_2O/CH_4 molar ratio of 4 at 873 K, H_2 at concentrations over 98% can be obtained all through fuel/steam feed stage. At the beginning of fuel/steam flow, $NiO_{reacted}/CH_4$ molar ratios are high (~ 3). Under these conditions, CO_2 concentrations would be very high in a process without CaO. However, in the presence of CaO sorbent, carbonation reaction is greatly enhanced at the beginning of fuel/steam feed, due to the great availability of CO_2, favoring the production of high purity hydrogen even at conditions under which NiO reduction reactions play an important role in the chemical mechanism. Comparatively, in absence of CaO sorbent, H_2 at concentrations of only 40 mol% are expected at the beginning of fuel flow. Thus, in the presence of a sorbent, with a suitable inlet H_2O/CH_4 molar rate, pure hydrogen can be produced continuously under fuel/steam feed at 873 K. Besides, the heat necessary for the steam reforming is provided by the carbonation reaction. In this way, the heat released during air flow can be entirely used to decompose the $CaCO_3$ into CaO. Therefore, with the USR technology, CaO can be regenerated under air flows, and an economically feasible process can be achieved. If $NiO_{reacted}/CH_4$ molar ratio reached at the end of fuel/steam stage is low (e.g. 0.12), a $CaCO_3/Ni$ molar ratio of ~ 0.7 can be used during air feed, which results in an overall auto-thermal operation. If

the duration of fuel/steam feed is not so long, and $NiO_{reacted}/CH_4$ molar ratio reached at the end of fuel/steam stage is greater (e.g. 1.22), a $CaCO_3/Ni$ molar ratio of 1.4 (maximum possible value) can be used. Although theoretical results suggest that high purity H_2 can be produced during long periods of auto-thermal operation, in practice, the period of pure hydrogen production will be limited by the CO_2 breakthrough curve of the sorbent.

- In the presence of CaO, lower temperatures are preferred. By increasing 100 K, H_2 production can be greatly decreased, because the carbonation reaction is very sensitive to temperature. At 973 K, CaO conversion decreases with time even at an inlet H_2O/CH_4 molar ratio of 4. In this case, the maximum H_2 concentration is 90 mol%, obtained in a narrow range of $NiO_{reacted}/CH_4$ molar ratios. Thus, at 973 K, H_2-rich gas is produced during shorter periods than at 873 K.

- At 873 K, with CaO sorbent, it is possible to obtain 3.7 moles of H_2 per mol of CH_4, using inlet H_2O/CH_4 molar ratios greater than 3.

- The generalized diagrams of concentration, selectivity, moles and enthalpy change as a function of inlet H_2O/CH_4 and $NiO_{reacted}/CH_4$ molar ratio can aid in monitoring and designing new experiments involving the USR and chemical looping reforming technologies.

- Future work will include a detailed thermodynamic analysis of the USR process with sulfur-containing fuels.

Acknowledgments

References

[1] W.H. Chen, M.R. Lin, J.J. Lu, Y. Chao, T.S. Leu, Int. J. Hydrogen Energy 35 (2010) 11787–11797.
[2] Y.S. Seo, A. Shirley, S.T. Kolaczkowski, J. Power Sources 108 (2002) 213–225.
[3] Y. Li, Y. Wang, X. Zhang, Z. Mi, Int. J. Hydrogen Energy 33 (2008) 2507–2514.
[4] L.F. de Diego, M. Ortiz, F. García-Labiano, J. Adánez, A. Abad, P. Gayán, J. Power Sources 192 (2009) 27–34.
[5] T. Mattisson, M. Johansson, A. Lyngfelt, Fuel 85 (2006) 736–747.
[6] R.K. Lyon, J.A. Cole, Combust. Flame 121 (2000) 249–261.
[7] V. Dupont, A.B. Ross, E. Knight, I. Hanley, M.V. Twigg, Chem. Eng. Sci. 63 (2008) 2966–2979.
[8] V. Dupont, A.B. Ross, I. Hanley, M.V. Twigg, Int. J. Hydrogen Energy 32 (2007) 67–79.
[9] F.-X. Chiron, G.S. Patience, Fuel (2011), doi:10.1016/j.fuel.2011.02.029.
[10] P. Pimenidou, G. Rickett, V. Dupont, M.V. Twigg, Bioresour. Technol. 101 (2010) 6389–6397.
[11] P. Pimenidou, G. Rickett, V. Dupont, M.V. Twigg, Bioresour. Technol. 101 (2010) 9279–9286.
[12] A. Lima da Silva, I.L. Muller, Int. J. Hydrogen Energy 36 (2011) 2057–2075.
[13] N. Hildebrand, J. Readman, I.M. Dahl, R. Blom, Appl. Catal. A: Gen. 303 (2006) 131–137.
[14] R.V. Kumar, J.A. Cole, R.K. Lyon, Preprints of Symposia, 218th ACS National Meeting, vol. 44, no. 4, August 22–16, New Orleans, LA, 1999, pp. 894–898.
[15] O. Knacke, O. Kubaschewski, K. Hesselmann, Thermochemical Properties of Inorganic Substances, second ed., Springer-Verlag, Berlin, 1991.
[16] A. Lima da Silva, C.F. Malfatti, I.L. Muller, Int. J. Hydrogen Energy 34 (2009) 4321–4330.
[17] A. Lima da Silva, I.L. Muller, J. Power Sources 195 (2010) 5637–5644.
[18] B. Dou, V. Dupont, G. Rickett, N. Blakeman, P.T. Williams, H. Chen, Y. Ding, M. Ghadiri, Bioresour. Technol. 100 (2009) 3540–3547.